

1 **Connectivity between spawning and nursery areas for Pacific cod (*Gadus***
2 ***macrocephalus*) in the Gulf of Alaska**

3

4 S. Hinckley^a, W.T. Stockhausen^a, K.O. Coyle^b, B.J. Laurel^c, G.A. Gibson^d, C. Parada^{e,f}, A.J.
5 Hermann^{g,h}, M. Doyle^a, T. P. Hurst^{c,*}, A. E. Puntⁱ, C. Ladd^h

6

7 ^a*Alaska Fisheries Science Center, National Marine Fisheries Service, NOAA, 7600 Sand Point Way, NE, Seattle,*
8 *WA 98115-6349*

9 ^b*Institute of Marine Science, University of Alaska, Fairbanks, AK 99775-7220*

10 ^c*Fisheries Behavioral Ecology Program, Alaska Fisheries Science Center, National Marine Fisheries Service,*
11 *NOAA, Hatfield Marine Science Center, Newport, OR 97365*

12 ^d*International Arctic Research Center, University of Alaska Fairbanks, PO Box 757340, Fairbanks, AK 99775*

13 ^e*Departamento de Geofísica, Universidad de Concepción, Casilla 160-C, Concepción, Chile*

14 ^f*Instituto Milenio de Oceanografía, Universidad de Concepción, Concepción, Chile*

15 ^g*Joint Institute for the Study of the Atmosphere and Ocean, University of Washington, Seattle WA 98195*

16 ^h*Pacific Marine Environmental Laboratory, NOAA, 7600 Sand Point Way NE, Seattle, WA 98115-6349*

17 ⁱ*School of Aquatic and Fishery Sciences, University of Washington, Seattle, WA 98195-5020, USA*

18

19

20

21 *Corresponding author. Phone: (o) 541-961-7297; (m) 541-961-7297; Fax: 541-867-0136

22 *E-mail address:* thomas.hurst@noaa.gov (T.P. Hurst)

23

24 **ABSTRACT**

25

26 We present the results of a study of the connectivity between Pacific cod spawning and
27 nursery areas, and settlement of Pacific cod in the Gulf of Alaska. This work was conducted to
28 address the hypothesis that spatial and temporal patterns of recruitment are related to variability
29 in connectivity between spawning and nursery areas. To examine this hypothesis, we developed
30 a Lagrangian, biophysical, individual-based model of Pacific cod early life history and dispersal
31 using the Dispersal Model for Early Life Stages (DisMELS) framework. This model is driven by
32 currents and scalars such as temperature from a version of the Regional Oceanographic Model
33 System (ROMS) developed for the Gulf of Alaska. Results of our study show connectivity
34 patterns predicted by the model that agree with our understanding (based on genetic analyses)
35 that there is a high degree of localized retention in Pacific cod. The results indicate that the
36 Shumagin Islands and Prince William Sound regions may serve as important collectors of Pacific
37 cod recruits from upstream spawning areas. We also find correlations between individual-based
38 model outputs and several large-scale climate indicators that appear to show settlement in several
39 important nursery areas, and recruitment overall, are positively affected by slower gyre
40 circulation in the Gulf of Alaska. We hypothesize that this is due to enhancement of retention,
41 settlement in the Shumagin Island region, and reduction of transport of young cod out of the Gulf
42 of Alaska to the southwest.

43

44 **Keywords:** USA, Alaska, Gulf of Alaska; *Gadus macrocephalus*, Pacific cod, Recruitment;
45 **Modelling**

46

47 **1. Introduction**

48

49 The Gulf of Alaska Integrated Ecosystem Program (GOAIERP) was a vertically-integrated
50 study of the physics, fisheries and ecosystem of the Gulf of Alaska (GOA). The goal of the
51 GOAIERP was to identify how physical and biological variability affect recruitment of five
52 commercially-important groundfish species in the Gulf. The main hypothesis of the GOAIERP
53 was that survival of young fish during transport from spawning to nursery areas influences
54 recruitment variability. Successful recruitment depends on many interrelated physical (runoff,
55 mixing, water temperature, and wind speed and direction) and biological (predation, food supply,
56 and competition) factors along the transport pathways. We refer to the biophysical environment
57 that individuals have to navigate during the first year of life as “the gauntlet.”

58 This paper focuses on Pacific cod (*Gadus macrocephalus*), one of GOAIERPs five focal
59 groundfish species. Pacific cod is a commercially important species in the GOA, accounting for
60 318,870 t or 14.7% of the total catch of Alaska groundfish in 2013 (Alaska Fisheries Science
61 Center, Seattle, WA, http://www.afsc.noaa.gov/species/Pacific_cod.php). Pacific cod are also a
62 key predator species in the GOA, especially on walleye pollock (Aydin et al., 2007). Cod are
63 opportunistic predators, and as such have a varied diet, feeding on fish and invertebrate species,
64 including commercially important crabs. They appear to be sensitive to bottom up effects from
65 both pelagic and benthic pathways (Aydin et al., 2007). Fishing, along with predation by
66 groundfish and marine mammals, accounts for most of the Pacific cod mortality in the GOA.

67 The abundance of Pacific cod in Alaskan waters has been highly variable. Spawning
68 stock biomass (SSB, Fig. 1) was high during the early 1980s due to a year of very high
69 recruitment of Pacific cod in 1977 (Barbeaux et al., 2018). SSB declined from the mid-1980s

70 until 2009, and then increased until 2014 when it experienced a significant decline during a
71 marine heat wave in the GOA (Di Lorenzo and Mantua, 2016). The cohorts of 1977 and 2012
72 were the strongest in recent decades, although the factors driving those recruitment events, and
73 recruitment variability in general, are not well understood. It has been recognized since the work
74 of Hjort (1914) that there is rarely a good relationship between spawning stock biomass of marine
75 fish species and recruitment, and that recruitment levels are the result of complex interrelationships
76 of physical and biological variables affecting early life stages (Houde, 2009). We hypothesize that
77 variability in patterns of connectivity, i.e. transport between spawning and nursery areas,
78 underlies variability in Pacific cod recruitment and we use a Lagrangian, spatially-explicit,
79 Individual Based Model (IBM) for Pacific cod to test it. The term “recruitment” (or “recruits”) in
80 this study refers to the number of age-0 Pacific cod at the end of their first year of life estimated
81 by the stock assessment model, as reported in the SAFE (Stock Assessment and Fisheries
82 Evaluation) document (Barbeaux et al., 2018).

83 Relative to their congener Atlantic cod (*Gadus morhua*), very little is known about the
84 dispersal and connectivity patterns of Pacific cod. Spawning Pacific cod are found in the GOA
85 between February and July (Dunn and Matarese, 1987). Eggs are demersal and semi-adhesive
86 (Laurel et al., 2008), which has been hypothesized to limit dispersal compared to the pelagic
87 eggs of Atlantic cod. Eggs are also stenothermal, euryhaline and euryoxic, with optimum
88 temperatures for development between 3.5 and 4°C (Alderdice and Forrester, 1971). At 4°C,
89 hatching occurs at 21-26 days after fertilization and newly hatched yolk-sac larvae are 3.8-5.3
90 mm SL (Laurel et al., 2008). The yolk-sac larval stage duration is between 3 and 12 days
91 depending on temperature (Laurel et al., 2008). Larvae are pelagic and yolk-sac larvae show a
92 strong surface orientation as early as 1 day post-hatch (Hurst et al., 2009). Larvae occur

93 primarily in the upper 45 m; however larval depths are highly variable. Flexion occurs at 20-35
94 days after hatch at 8° C (Narimatsu et al., 2007). After flexion (10-17 mm), larvae respond to
95 light variation with vertical movements reflecting a diel vertical migration with greater occupied
96 depths during the day (Hurst et al., 2009), although this pattern was not observed by Brodeur and
97 Rugen (1994). Transformation to the juvenile stage occurs at around 25-35 mm SL, about 70-75
98 days after hatch at 8° C. Although maturity occurs at 4-5 years of age, for our purposes,
99 “juvenile” explicitly refers to fish during their first year of life. By July of their first year,
100 individuals have been transported towards shore (Rugen and Matarese, 1988), and have begun to
101 settle to the bottom. Juvenile nursery areas are primarily shallow coastal embayments (Abookire
102 et al., 2007; Laurel et al., 2007). Although juveniles have been caught at depths to 70 m (Smith
103 et al., 1984), densities are generally highest in waters shallower than 20 m during the summer
104 and fall (Laurel et al., 2009). Within this depth region, juvenile cod show a preference for high
105 salinity water (Abookire et al., 2007) and structured habitat features (e.g. sea cucumber mounds,
106 eelgrass and kelp; Laur and Haldorson, 1996; Dean et al., 2000; Laurel et al., 2007). Pacific cod
107 are known to make annual feeding migrations and return to prior spawning locations, but some
108 stock components may be non-migratory. Genetic studies indicate that dispersal distances of
109 Pacific cod between birth and reproduction may be less than 30 km (Cunningham et al., 2008).

110 Mean circulation in the GOA is predominantly east to west. Along the continental shelf
111 break the Alaskan Stream is a westward flowing boundary current with flow rates up to 80-100
112 cm s⁻¹ (Reed and Schumacher, 1984). On the shelf, within about 50 km of the coast, the Alaska
113 Coastal Current is a westward-flowing, wind-driven current (Royer, 1998; Stabeno et al., 2016)
114 with a low salinity core and flow rates of 25 to 175 cm s⁻¹ (Stabeno et al., 1995). Both current
115 systems meander and shed eddies, which affect the trajectories and mixing of water masses

116 (Janout et al., 2009; Ladd and Stabeno, 2009; Ladd et al., 2005; Okkonen, 2003). Storms
117 associated with the Aleutian Low atmospheric pressure system promote onshore advection of
118 surface water (Cooney, 1986), and the coastal mountain range constrains these pressure systems
119 resulting in elevated precipitation and runoff (Royer, 1982). Variation in the storms and runoff
120 result in interannual variability in many aspects of the circulation including onshore advection
121 (Stabeno et al., 2004).

122 IBMs, such as that used here, are biophysical models that have been used in studies of
123 recruitment (Hinckley et al., 1996, Stockhausen and Lipcius, 2003), marine reserves
124 (Stockhausen and Hermann, 2007; Stockhausen and Lipcius, 2001; Stockhausen et al., 2000;
125 Pelc et al., 2010; Paris et al., 2004), and connectivity (Cowen et al., 2006, Cowen et al., 2007,
126 Cooper et al., 2013, Parada et al., 2010), and for other applications in marine ecology and
127 fisheries. These models generally include several pelagic early life history stages, with biological
128 processes that differ among the stages. IBMs are typically coupled to regional three-dimensional
129 oceanographic models to simulate the environmental factors that affect development and
130 transport of each life stage such as temperature, salinity, and currents. IBMs can be simple,
131 accounting for only a few base variables, or relatively complex, to include a full suite of
132 processes such as feeding, bioenergetics, growth and movement (e.g. Werner et al., 2001, North
133 et al., 2009, Hinckley et al., 1996; Hinckley et al., 2001; Megrey and Hinckley, 2001, Kim et al.,
134 2015, Parada et al., 2010). The degree of complexity often reflects the data available for a
135 particular species as well as the research question or focus.

136 Using a model-based approach to explore ways in which environmental variability in the
137 GOA affects recruitment of Pacific cod, we specifically address the hypothesis that *Recruitment*
138 *variability of Pacific cod is primarily influenced by variability in the proportion of young fish*

139 *transported from (offshore) spawning areas to nearshore nursery areas (connectivity) due to*
140 *interannual differences in the characteristics of the physical regime in the GOA.* To address our
141 hypothesis, we initially examine connectivity between potential Pacific cod spawning and
142 nursery areas and patterns of settlement, and then develop model-based indices of connectivity to
143 compare with indices of environmental variables that could impact young Pacific cod. These
144 potential indices are then compared to variability in recruitment estimates from the stock
145 assessment of Pacific cod.

146

147

148 **2. Methods**

149

150 *2.1. Model descriptions and simulations*

151

152 We used a species-specific IBM coupled to a hydrodynamic model of the region to
153 explore Pacific cod connectivity in the Gulf of Alaska. The structure of the IBM is similar to
154 those developed for walleye pollock (Hinckley et al., 1996; Hinckley et al., 2016; Parada et al.,
155 2016) and for snow crab (Parada et al., 2010) in that it is driven by a 3-dimensional (3D)
156 hydrodynamic model and describes biophysical processes happening during early life history
157 stages. However, it uses a different modeling framework than the earlier models, and stage
158 processes and parameters are specific to Pacific cod. The walleye pollock and snow crab models
159 used the Ichthyops framework (Lett et al., 2008). The current model was developed within the
160 Dispersal Model for Early Life Stages (DisMELS) framework that uses the output of a coupled,
161 biophysical, Regional Oceanographic Model System (ROMS) to provide information on the

162 physical and lower trophic level environment. The coupled model simulation years were 1997 to
163 2013. This time span includes the field sampling years of the GOA IERP (2011-2013), years of
164 high and low recruitment of Pacific cod, and years representing different climate conditions
165 (including the 1997-1998 El Nino).

166

167 2.1.1. *ROMS Hydrographic Model*

168 We employed two model domains: a 3-km resolution model of the GOA, embedded
169 within an 11-km resolution model of the Northeast Pacific. The hydrodynamic models are based
170 on ROMS (Shchepetkin and McWilliams, 2005; Haidvogel et al., 2008), version 3. ROMS is a
171 hydrostatic, primitive equation ocean model that utilizes sigma-coordinates in the vertical and
172 curvilinear orthogonal coordinates in the horizontal. The 3-km and 11-km regional models each
173 utilized 42 vertical layers, with refinement for tighter spacing to resolve the surface boundary
174 layer.

175 The 3-km grid extends from northern British Columbia in the east to west of the
176 Shumagin Islands off the Alaska Peninsula in the west, and from the coast to approximately 1200
177 km offshore, with ~500 x 500 grid points. The 11-km model domain covers the region from Baja
178 California to the Chukchi Sea, from the coast to approximately 2000 km offshore, for a total of
179 ~200 x 500 grid points. Fine-scale bathymetry is based on ETOPO5, a gridded data set of land
180 and sea-floor elevations (NOAA, National Geophysical Data Center, Boulder, Colorado, 1988)
181 and supplementary datasets as described in Danielson et al. (2011); smoothing of the bathymetry
182 was utilized for numerical stability. The layered coordinate system of ROMS required that
183 regions shallower than 10 m be set to a depth of 10 m to ensure numerical stability (which would
184 be violated for overly thin layers, given a fixed model time step). Vertical mixing in both the 3-

185 km and 11-km models was based on the algorithms of Large et al. (1994). Tidal dynamics are
186 included in the 3-km ROMS model; the explicit inclusion of tidal flows allows tidally-generated
187 mixing and tidal residual flows to develop. Tides are included in the 11-km model simulation.

188 The models were forced by 6-hourly atmospheric (for surface forcing) and monthly
189 oceanic (for initial and boundary conditions) reanalysis output from NOAA's global Climate
190 Forecast System Reanalysis (CFSR; Saha et al., 2010), and subsequent operational analyses,
191 spanning the years 1995-2013. Horizontal resolution of the CFSR atmospheric and oceanic
192 reanalyses is ~ 40 km; these were interpolated to the regional grids. Bulk forcing, based on the
193 algorithms of Large and Yeager (2008), was used to relate the 6-hourly CFSR atmospheric
194 variables (wind velocities, air temperature, rainfall rate, absolute humidity, downward shortwave
195 and longwave radiation) to surface stress and the net transfers of sensible heat, latent heat,
196 shortwave and longwave radiation through the sea surface, as well as surface freshening by the
197 rainfall.

198 The oceanic boundary conditions were enforced using the hybrid nudging/radiation
199 scheme of Marchesiello et al. (2001). The 11-km model initial and boundary conditions were
200 derived from the CFSR, while these conditions for the 3-km model were derived from weekly
201 averages of the 11-km model physical output, spatially interpolated onto the 3-km model
202 boundaries (one-way nesting with no feedback to the outer model). The 11-km model was run
203 for one year prior to its use for initialization of the 3-km model.

204 Freshwater runoff was applied to the northern Gulf of Alaska simulations by freshening
205 surface salinity within a few grid points of the coastline using an exponential taper based on
206 squared distance from the coastline, with an e-folding distance of ~30 km. This technique
207 minimized the runaway stratification artifact, which has been observed using continuous

208 horizontal input of freshwater along broad stretches of the coastline (Dobbins et al., 2009; Vaz
209 and Simpson, 1994). The alongshore spatial pattern of the runoff for the 11-km NEP grid for
210 1995 – 2007 came from Dai et al. (2009). After 2007, a climatology based on Dai et al. (2009)
211 was used to set the NEP grid runoff. Runoff for the 3-km CGOA grid was generated from a high-
212 resolution freshwater discharge model for the Gulf of Alaska (Hill et al., 2015; Beamer et al.,
213 2016) as described in Coyle et al. (in press, this volume).

214 Output from the 3-km model was lowpass-filtered to eliminate tidal and inertial
215 oscillations, and stored as 1-day averages for subsequent use by the IBMs. Validation studies and
216 descriptions of related versions of the 11-km NEP model are available in Danielson et al. (2011)
217 and Hermann et al. (2009a). Validation studies and descriptions of related versions of the 3-km
218 biogeochemical and physical GOA model are described in Hermann et al. (2009b), Hinckley et
219 al. (2009), Dobbins et al. (2009), and Coyle et al. (2012, 2013).

220

221 2.1.2. *DisMELS framework*

222 DisMELS was developed at the Alaska Fisheries Science Center (NOAA/NMFS) to
223 provide a framework to develop and run IBMs simulating the early life stage development and
224 dispersion of marine fishes and invertebrates with pelagic egg and larval stages. It couples an
225 IBM framework with stored output from a ROMS model to provide a time-varying, 3D physical
226 environment in which to simulate the dispersal trajectories of thousands of simulated eggs and
227 larvae from natal locations up to early juvenile life stages. DisMELS also provides a graphical
228 user interface to facilitate defining life stage sequences, stage-specific characteristics, and initial
229 conditions, as well as to run models and analyze results.

230

231 *2.1.3. The Pacific cod IBM*

232 A conceptual model of Pacific cod early life history is shown in Fig. 3. Six life stages were
233 included in the IBM (eggs, yolk-sac larvae, pre-flexion feeding larvae, post-flexion feeding
234 larvae, epipelagic juveniles and settled juveniles). Processes such as growth and development,
235 depth distribution, and diel migration differed by life stage. To accommodate the complexity of
236 Pacific cod life history, changes and additions were made to the basic DisMELS model code to
237 include parameters and algorithms specific to Pacific cod egg, larval and juvenile (less than one-
238 year old) stages. The stage-specific parameterization of the IBM is described below.

239

240 *2.1.3.1. Egg stage*

241 Pacific cod spawn at the sea bottom over the continental shelf; therefore, eggs were
242 considered to be attached to the bottom and do not move from their spawning location. The
243 initial size of embryos in the model was assumed to be 0 mm, and using growth rates for
244 embryos (Hurst et al., 2010) resulted in size at hatch averaging between 4 and 5 mm (Laurel et
245 al., 2008; Doyle and Mier, 2016). Egg stage duration was modeled as a function of temperature
246 (Laurel et al., 2008) with a minimum set to 8 d and an average of 20-25 d.

247

248 *2.1.3.2. Yolk-sac stage*

249 Upon hatching, yolk-sac larvae move quickly to the surface (Matarese et al., 1989;
250 Mecklenburg et al., 2002; Hurst et al., 2009, Doyle and Mier, 2016). The depths for yolk-sac
251 larvae were restricted to 0-40 m (Brodeur and Rugen, 1994). Yolk-sac larvae were assumed to
252 move vertically in a random manner with a mean vertical velocity of $1 \times 10^{-4} \text{ m s}^{-1}$. Progress
253 through the yolk-sac larval stage was modelled similar to walleye pollock (Hinckley et al.,

254 1996). The number of days to the point of no return (PNR), the time at which a larva cannot
255 recover from starvation, was a function of temperature (Laurel et al., 2008), as were days to
256 yolk-sac absorption (YSA) or first-feeding readiness. If larval time in the stage was less than
257 YSA, larval age and growth were incremented and feeding did not occur. Once a larva was ready
258 to feed (past YSA), the probability of feeding on each day was set to a random variate between 0
259 and 1, which increased linearly with age. If it did feed, larval age and growth were incremented
260 using the growth algorithm for the yolk-sac stage, and the larva passed into the pre-flexion
261 feeding larval stage. If it did not feed, age and growth were incremented, but it did not pass into
262 the next stage. If PNR was reached without feeding, the larva died of starvation. The duration of
263 the yolk-sac larval stage was constrained to 2 – 15 days.

264

265 *2.1.3.3. Pre-flexion feeding larvae through benthic juvenile stages*

266 During the pre-flexion feeding larval stage, the individual's depth was constrained to
267 between 0 and 40 m, and there was no diel migration (Brodeur and Rugen, 1994; Hurst et al.,
268 2009). Vertical velocity was a function of length and temperature (Ottmar and Hurst, 2012).
269 Growth rates for pre-flexion stages were based on measurements in Hurst et al (2010). In that
270 paper, the authors acknowledge the potential for underestimation of growth rates due to the use
271 of rotifers instead of natural copepods as prey. However additional runs of our model applying
272 elevated pre-flexion growth rates led to similar patterns of connectivity between spawning and
273 nursery areas.

274 Each larva passed into the post-flexion feeding larval stage after reaching a length of 13.5
275 mm (Matarese et al., 1989). Growth rate for the post-flexion feeding larval stage differed from
276 that of the previous stage (Hurst et al., 2010) and diel migration was initiated. Daytime depth

277 varied between 20 and 40 m, whereas nighttime depth was between 0 and 20 m. The day-night
278 depth pattern was based on maintaining the 0-40 m depth range observed for pre-flexion larvae
279 (Brodeur and Rugen, 1994) as well as the vertical migration behavior observed in lab
280 experiments (Hurst et al., 2009). Each larva grew until it reached the length of transformation (25
281 mm, Dunn and Matarese, 1987), when it passed into the epipelagic juvenile stage. Larvae in this
282 developmental stage exhibited a similar pattern of day and night depths and vertical velocity as
283 the preceding stage, but could settle if they reached an area where the depth was less than 70 m
284 (Smith et al., 1984). Individuals in the benthic juvenile stage were constrained to one location
285 (although they actually move horizontally in an unknown manner). The goal of this study was to
286 model transport to potential settlement regions, and was not focused on fine-scale post-
287 settlement habitat selection, hence the lack of movement after settlement.

288 Growth rates for all life stages were functions of temperature and were taken from Hurst
289 et al. (2010); these growth rates differed by life stage (Table 1). Except for starvation during the
290 first-feeding stage, there was no explicit mortality included in the IBM. This is because there are
291 insufficient data on predator feeding habits, distribution and abundance, or on the total
292 abundance of cod early life stages necessary to parameterize predation mortality. This
293 simplification implies that the connectivity shown here represents maximum connectivity
294 between potential spawning and nursery areas. However, the main purpose of this study was to
295 examine stability and variation in the oceanographic drivers of dispersal and connectivity
296 patterns. Parameters and algorithms used in the IBM are listed in Table 1.

297

298 *2.2. Connectivity*

299

300 Connectivity between zones was defined as the fraction of fish initiated in a specific
301 spawning area that ended in each zone. We divided the GOA into geographical zones
302 representing source (spawning, zones 102-113, 202-213) and sink or ending (nursery, zones 101-
303 113, and other non-nursery (0-12, 201-213) areas (Fig. 2), to assess the connectivity between
304 spawning and nursery (or other) areas. Individuals that left the ROMS grid were classified as
305 ending in zone 998. The GOA was divided into 12 alongshore zones, and several depth zones.
306 These zones, by discretizing space in the GOA, help us define where each individual spawns,
307 zones that it may travel through, and the zone where it settles. The zones also facilitate the
308 analysis of connectivity by grouping the locations of individuals. The alongshore zones were
309 defined based on several criteria, including topography and geographic region (e.g. Cook Inlet or
310 West Shumagins). The depth zones represented depths significant to Pacific cod life history.
311 Pacific cod spawning zones were considered to be between 20 and 200 m depth (Dunn and
312 Matarese, 1987) while nursery areas were assumed to be regions where the depth was less than
313 70 m (Smith et al., 1984).

314

315 *2.3. Initial conditions*

316

317 Little information on specific locations of Pacific cod spawning or egg distribution exists.
318 Pacific cod spawning distribution is known to be patchy, but the specific locations of these
319 patches are not known. The few studies of distribution of Pacific cod spawning adults in the Gulf
320 of Alaska (Stark, 2007; Hirschberger and Smith, 1983; Fisheries Monitoring and Analysis
321 Division, Alaska Fisheries Science Center, NMFS, Seattle, unpublished data) have narrow
322 spatial and temporal coverage. Commercial catch between February and June (the spawning

323 period) occurs throughout the Gulf of Alaska and is not specifically targeted on the spawning
324 aggregations, so could not be used to delineate spawning patches. Furthermore, because of their
325 demersal nature, Pacific cod eggs are not caught in ichthyoplankton surveys which use pelagic
326 nets (Dunn and Matarese, 1987). Due to this paucity of information, cod eggs were released over
327 all suitable locations in the GOA where the water depth was shallower than 200 m.

328 A sensitivity analysis was performed to determine the optimal spatial resolution for
329 initialization of individuals. For this test, we released eggs from two connectivity zones
330 (different zones from those shown in Fig. 2) in Southeast Alaska, a shallow (<70 m) spawning
331 zone and a deep (70-200 m) spawning zone. Within these zones, eggs were released on grids
332 with spatial resolutions of 1, 2.5, 5, 7 and 10 km, with a single egg released at each grid point.
333 Eggs were released on 15 March at the bottom, and individuals were tracked until 1 November.
334 At the end of each simulation, the final connectivity zone of individuals was determined and
335 connectivity zones were ranked by the number of individuals they contained. The top ten final
336 zones (of 36) and the total number of individuals simulated (which is determined by the grid
337 size) were compared for each grid size (Table 2). Grids with larger spatial resolutions were
338 compared to the 1 km grid. Grids with spatial resolutions of 1 km and 2.5 km resulted in the
339 same top 10 final zones, although these were in a somewhat different order. Nine zones were the
340 same (out of the top 10) for the 5- and 7-km grids as were found for the 1-km grid, and the 10-
341 km grid resulted in eight zones that were the same as the 1-km grid. The simulations with the 1-
342 km and 2.5-km grids required substantially more modelled individuals than the coarser grids.
343 Final models were run releasing eggs on a 5-km grid, which provided agreement with the finer 1-
344 km grid results with markedly reduced computation time.

345 Individuals were released mid-month from February to June on the 5-km grid. The June
346 release resulted in no settlers by the end of the simulation (31 October), so this release time was
347 removed from further analysis. Due to the narrow shelf and small areal extent of potential
348 spawning areas in regions 101 and 201, no eggs were released in these zones.

349

350 *2.4. Analysis methods*

351

352 *2.4.1. Connectivity matrices*

353 Connectivity matrices were computed for each year of the simulation. The cells of the
354 matrices show the probability of modelled individuals from each spawning zone dispersing to
355 any connectivity zone by the end of the simulation (so that the sum of the probabilities over each
356 row of the matrix (spawning areas) is 1.0). The ending zones (columns of the matrix) could be
357 nursery areas (<70 m), or any other zone. Individuals that exited the 3-km grid (designated as
358 Zone 998) were also recorded. The average probability of transport from a specified start zone to
359 a specific end zone and the standard deviation (SD_{conn}) of these probabilities over all simulated
360 years (1996-2011) were calculated. The average and SD_{conn} were plotted as matrices, and the
361 spawning areas for settlement regions of interest were plotted to clarify some of the observed
362 patterns.

363 We hypothesize that variability in annual recruitment is related to variability in
364 connectivity. We used a Normalized Difference Index (*NDI*) and an Overlap Coefficient (*OC*) to
365 examine this hypothesis. The *NDI* and the *OC* have been applied to compare modelled
366 distributions with observed field distributions of young fish (Hinckley et al., 2016).

367

368 2.4.2. *Normalized difference index*

369 The normalized difference index (*NDI*) was adapted from Hinckley et al. (2016),
370 Berntsen et al. (1996) and Sjøiland and Skogen (2000), and used to examine variation among
371 annual connectivity matrices. We calculated the normalized difference between modelled
372 connectivity matrix probabilities for each *i*-th cell for each year *t* ($P_{i,t}$) and the average modelled
373 connectivity matrix values for all years for each *i*-th cell (\bar{P}_i), divided by the standard deviation
374 (SD_i) of modelled connectivity output for all years for each cell. Following Sjøiland and Skogen
375 (2000), we used the maximum of either the SD_i or 0.01 to avoid division by a very small number.
376 The resulting cost function field $NDI_{i,t}$ is defined by:

$$377 \quad NDI_{i,t} = (P_{i,t} - \bar{P}_i) / \max(SD_i, 0.01) \quad (10)$$

378 Negative values of $NDI_{i,t}$ indicate that the connectivity probability for that cell/year was less than
379 the mean connectivity probability for that cell, whereas positive values of $NDI_{i,t}$ indicate that the
380 connectivity probability for that cell/year was greater than the mean. The NDI_t for each year is
381 the sum of the absolute values over all cells with higher NDI_t values indicate greater differences
382 from the overall mean pattern in connectivity. The time series of NDI_t values was compared to
383 the recruitment time series for Pacific cod.

384

385 2.4.3. *Overlap coefficient*

386 An overlap coefficient (*OC*) was used to examine the overlap of each year's connectivity
387 matrix with the average (1997-2013) connectivity matrix. This type of coefficient is normally
388 used to examine the overlap of spatial distributions (Hinrichsen et al., 2005); here we apply it to
389 connectivity matrices calculated as:

$$390 \quad OC_t = 2 \sum_{i=1}^n (P_{i,t} \cdot \bar{P}_i) / (\sum_{i=1}^n P_{i,t}^2 + \sum_{i=1}^n \bar{P}_i^2)$$

391 for year t and cell i . The OC is 0 when there is no overlap and 1 when the two matrices are
392 identical. Hinckley et al. (2016) used this index to compare modelled distributions of pollock
393 larvae with survey distributions. Hinrichsen et al. (2005) applied OC to determine how many
394 modelled larvae and prey were simultaneously present in the subareas of the central Baltic Sea.

395

396 2.4.4. *Settlement analysis, physical indices and recruitment*

397 We examined several other metrics: (1) the fraction of the total number of simulated
398 individuals that settled by year, (2) the fraction settling in each nursery zone, and (3) the fraction
399 settling from each spawning zone. Several model-derived time series were compared to Pacific
400 cod recruitment (Barbeaux et al., 2018) using Pearson's correlation coefficient. We examined the
401 correlations (Pearson's r) between the fraction settling in each nursery zone and several large-
402 scale climate indices. An average of three winter months (December-February), just prior to
403 spawning, was used for each index. The Multivariate ENSO index (MEI, Wolter and Timlin,
404 1993, 2011) reflects the El Niño/La Niña state with positive values representing stronger gyre
405 circulation associated with El Niño, and vice-versa for La Niña. The North Pacific Index (NPI,
406 Trenberth and Hurrell, 1994, 1995) is the area-weighted sea level pressure over the region
407 between 30°N and 65°N with positive NPI values reflecting a weaker Aleutian Low and reduced
408 gyre circulation. The Pacific Decadal Oscillation (PDO, Mantua et al., 1997; Zhang et al., 1997;
409 Bond and Harrison, 2000) represents Sea Surface Temperature (SST) anomalies in the North
410 Pacific. Lastly, the Arctic Oscillation (AO, Higgins et al., 2001, 2002) reflects the strength of
411 counterclockwise winds at ~55°N latitude, with negative AO values associated with increasing
412 storminess in mid-latitudes. The MEI, NPI and AO indices were chosen because they relate to
413 different drivers of circulation, and therefore larval transport, in the Gulf of Alaska. Stachura et

414 al. (2014) found that the NPI may be a good predictor of recruitment for fish species in the GOA.
415 The PDO was chosen because temperature affects growth of individuals in the Pacific cod IBM.
416 Growth determines larval life stage and therefore depth, which affects transport in a vertically
417 stratified ocean.

418

419

420 **3. Results**

421

422 *3.1. Connectivity*

423

424 The average annual connectivity for Pacific cod between spawning areas and ending
425 areas (including nursery and non-nursery areas) for the years 1997-2013 is shown in Fig. 4. For
426 modelled individuals initialized in the shallow (< 70 m) spawning areas, retention (i.e. settlement
427 in the same areas as release) of modelled individuals was the dominant pattern (average
428 probability =0.41). This pattern is indicated by the lower diagonal white line in Fig. 4. Some
429 young Pacific cod moved from their spawning areas to nearby areas downstream, as shown by
430 the shaded cells immediately left of the diagonal. Another important pattern was the movement
431 of individuals from deep spawning areas to adjacent inshore nursery areas (upper diagonal white
432 line in Fig, 4). However, the probabilities of such shoreward transport were less than the
433 probabilities of retention. For the most part, the early life stages of Pacific cod were not
434 transported great distances between spawning zones and nursery areas. Despite the general
435 pattern of retention, a high proportion of individuals were transported out of the GOA model
436 domain (designated as zone 998 on the connectivity matrices). The probability of loss was

437 between 0.01 and 0.91 (depending on the start zone) and was greatest for fish spawned to the
438 west of Kodiak Island (especially the deeper spawning areas 209-212; Fig. 2). Most of these
439 individuals were transported out of the model domain to the southwest; however, some were
440 transported out of the model grid to the southeast.

441 The largest standard deviation (SD_{conn}) in the probability of transport between start/end
442 pairs over the modelled years was 0.10 (Fig. 5). The highest variability in connectivity was seen
443 in the transport of individuals released in areas 112, 113, and 212 near the Shumagin Islands and
444 in fish transported out of the southwest corner of the grid.

445 The spawning areas for several of the nursery or ending regions and for the modelled
446 individuals that left the GOA are plotted to reflect an alternate perspective on dispersal (Fig. 6).
447 Retention in the spawning area is clearly the most important source for settling individuals in
448 each nursery area. The contribution of spawning zones to the east of the nursery area (102 and
449 202 being the farthest east) decreased rapidly with distance from the nursery area. Individuals
450 generally did not come from zones west of the settlement area (112 and 212 being the farthest
451 west). Area 106 (Prince William Sound) was more strongly connected to multiple spawning
452 areas upstream and offshore than other nursery areas. This was also true for nursery area 112
453 (West Shumagins). It is also clear from Fig. 6 that most individuals exiting the grid (Area 998)
454 came from the southwesterly spawning areas (112, 211,212) closest to the southwestern grid
455 boundary.

456

457 *3.2. Normalized difference index and overlap coefficient*

458

459 The year with the lowest *NDI*, i.e. the year in which connectivity patterns were most
460 similar to the mean, was 2000 (*NDI* = 20.50, Fig. 7). The year with the highest overall *NDI* (i.e. a
461 connectivity matrix most divergent from the mean) was 1998 (*NDI* = 36.45). The range of the
462 *OC* index was small. The year with the lowest *OC* (Fig. 7) was 1998 (*OC* = 0.94), and 2000 was
463 the year with the highest *OC* (0.98). *NDI* and *OC* were inversely correlated with $r = -0.84$ ($p <$
464 0.001).

465 The largest differences in 1998 from the annual mean were that more simulated
466 individuals exited the model domain (sink area 998) from areas 110 (Chirikof) and areas 207-211
467 (Kenai to East Shumagins, deep spawning areas) (Fig. 8). There was also higher than average
468 retention within area 103 (Cross Sound), and fewer individuals ending in area 112 (West
469 Shumagins) in that year. Recruitment of Pacific cod in 1998 was the second lowest of the
470 modelled period.

471

472 *3.3. Settlement, physical indices and recruitment*

473

474 The analysis of settlement fractions in each nursery zone must be considered preliminary,
475 as there is little information about initial spawning distributions. However, given this constraint,
476 settlement fractions (of the total number of simulated individuals) generally increased from east
477 to west with a peak in area 112 (West Shumagins, Fig.9A). The lowest fractions settled were in
478 Southeast Alaska (areas 101-103) and Yakutat/Icy Bay in East Central GOA (104-105).
479 Fractions settled in the central GOA from Prince William Sound (106) to Chirikof (110) regions
480 were similar and higher than those farther east.

481 The patterns of settlement for fish starting from the shallow and deep spawning areas
482 (Figs. 9B, C) were similar, and were quite high except for area 112 and 212 (West Shumagins).
483 The latter is probably because (as was mentioned in the connectivity results) Pacific cod are
484 mostly either retained in their spawning areas, or they disperse a short distance from their
485 starting location; in the case of area 212 they can easily move out of the grid to the southwest, as
486 the prevailing currents take them in this direction. Settlement fractions for individuals from
487 spawning areas 102-108 and 203-208 (Sitka to North Kodiak) were above 70%. Settlement
488 fractions decline from North Kodiak Island to the West Shumagins (areas 109-112 and 209-212).
489 Settlement of modelled individuals released in Cook Inlet (areas 113 and 213) was high (>80%).
490 It is unknown whether there is a high abundance of Pacific cod spawning in Cook Inlet. Of the
491 simulated years, 1998 had the lowest fraction settled (Fig. 9D) with 2003 and 1997 showing the
492 highest fraction settled.

493 Most of the model-derived time series that were compared to actual Pacific cod
494 recruitment from the NMFS stock assessments showed very low correlation coefficients (Table
495 3). However, the fraction settled in area 105 (Icy Bay) was positively correlated with observed
496 Pacific cod recruitment (as estimated by Barbeaux et al., 2018). Recruitment was negatively
497 correlated with settlement in areas 101 (Pt. Wales Island), 107 (Kenai), and 108 (North Kodiak).
498 Settlement in area 112 (West Shumagins) was negatively correlated with the MEI and NPI,
499 whereas settlement in area 105 was negatively correlated with the PDO. The AO index was not
500 significantly correlated with settlement in any of the nursery zones.

501

502

503 **4. Discussion**

504

505 Knowledge of connectivity, the linkage between spawning areas and settlement areas,
506 can increase our understanding of the fate of fish spawned in particular regions, of the potential
507 importance of different spawning and nursery areas, of stock structure, and of the impacts of
508 larger scale climate forcing on recruitment patterns. It can also give insight into how these
509 patterns may differ between the eastern and the western GOA, or of how these two regions may
510 be linked via larval transport. We hypothesized that variation in annual recruitment is related to
511 patterns of dispersal and connectivity throughout the Gulf of Alaska. Lagrangian IBMs are one
512 of the few available tools for studying connectivity, with their ability to follow modelled
513 individuals along transport pathways.

514 This study of connectivity and settlement patterns of Pacific cod in the Gulf of Alaska
515 revealed some general patterns that are in accordance with what is known about Pacific cod early
516 life history, and that also extend our understanding of potential transport and settlement patterns.
517 Some possible causes of variability in these patterns due to large-scale climate factors, and
518 consequences of these patterns and their interannual variability on recruitment were also
519 examined.

520 The results of modelled connectivity patterns indicate that the early life history stages of
521 Pacific cod generally do not disperse far from their natal areas. Retention of modelled
522 individuals in areas where they were spawned was the strongest connectivity pattern seen. This
523 result agrees with patterns of genetic variation suggesting limited dispersal rates in this species
524 (Cunningham et al., 2008). We also found that individuals spawned in shallower spawning areas
525 nearer to shore or in areas where the circulation is weaker are more likely to be retained than

526 those released in deeper shelf areas where strong directed currents such as the Alaska Current are
527 dominant, as might be expected. Many cod that were spawned to the west of Kodiak in the
528 model, especially in the Shelikof Strait sea valley (with its strong westward currents), were
529 transported out of the GOA. However, many modelled individuals were also transported from
530 the deeper shelf spawning regions to nearby nearshore settlement regions, indicating the
531 importance of cross-shelf transport. The variability in connectivity for Pacific cod was not as
532 high as for other, long-distance dispersing species such as sablefish (*Anoplopoma fimbria*,
533 Gibson et al., in press, this volume), Pacific Ocean perch (*Sebastes alutus*, Stockhausen et al., in
534 press, this volume) or arrowtooth flounder (*Atheresthes stomias*, Stockhausen et al., in press, this
535 volume). The highest variability was in the patterns that showed the strongest connections, such
536 as retention and transport out of the GOA. This restricted transport of early life stages of Pacific
537 cod has consequences for east vs. west differences. Cod spawned in southeast Alaska that were
538 not retained in that area, for example, were not likely to be transported much farther west than
539 Prince William Sound.

540 The retention and limited transport in our model results is partially because (in the model
541 and *in situ*) Pacific cod eggs are attached or semi-attached to the bottom for nearly a month of
542 their early life. This trait, which is unique among species in the genus may, among other things,
543 be an adaptation to restrict larval dispersal. In the model, we also assumed that once the
544 modelled individuals settle as benthic juveniles, they do not move from their settlement location.
545 Benthic juveniles cod are likely to move horizontally to some degree. However, it is thought that
546 they may not move far based on nearshore settlement dynamics of Atlantic cod (Laurel et al.,
547 2003).

548 The fraction of settling Pacific cod in these simulations was higher than that observed for
549 sablefish (Gibson et al., in press, this volume), Pacific Ocean perch and arrowtooth flounder
550 (Stockhausen, et al., in press, this volume). Walleye pollock settlement fractions are generally
551 between those for Pacific cod and the other species (Parada et al., 2016). We did not have precise
552 locations of Pacific cod spawning or information on the spatial pattern of predation on egg and
553 larval stages, so the number of individuals settling in each modelled nursery area may differ from
554 the dispersal patterns reflected here. However, the modelling results indicate that the area around
555 and just west of the Shumagin Islands could represent a significant nursery area for Pacific cod
556 in the Gulf of Alaska because this area received settling fish from a wide range of potential
557 spawning locations. Doyle and Mier (2016) show that many late larval Pacific cod concentrated
558 in this region in May. High commercial catches of adult Pacific cod are also found in this region
559 (<http://www.afsc.noaa.gov/maps/FMA/datamap/obsmap.html>).

560 Nursery areas in southeast Alaska and the east central GOA had the lowest settlement
561 rates and the highest likelihood of individuals spawned there being dispersed downstream or
562 offshore. This is likely due to the narrowness of the continental shelf, and the impingement of the
563 Alaska Current and oceanic eddies. A high proportion of modelled fish released in Cook Inlet
564 reached suitable settlement sites, but little is known about the magnitude of spawning activity
565 occurring there. Prince William Sound and the West Shumagins seem to act as collection areas
566 for fish transported from upstream areas. Individual fish from southeast Alaska to Prince William
567 Sound settled in Prince William Sound, as well as being retained in their spawning areas.
568 Individuals from Kodiak to the West Shumagins settled in the West Shumagins, as well as being
569 retained near their spawning areas. These results may indicate that if recruitment of Pacific cod is
570 determined in the early life stages, the eastern and western regions could show different

571 recruitment patterns. We were unable to examine this hypothesis however, because estimates of
572 recruitment for this species are made Gulf-wide, not for specific regions.

573 The year 1998 exhibited the highest divergence (using the *NDI*) from the mean
574 connectivity pattern, and had the lowest fraction settled of all years in our time series.
575 Recruitment in 1998 was also the third lowest of our modelled period. More modelled
576 individuals exited the GOA, and fewer individuals settled in West Shumagins in 1998.
577 Settlement in the east central GOA was positively correlated with recruitment, whereas
578 settlement around North Kodiak and the Kenai area was inversely correlated with recruitment,
579 although the reasons for the latter are unclear.

580 Several hypotheses arise from this work that require further exploration. For example,
581 settlement and recruitment success for Pacific cod may increase when the GOA gyre circulation
582 is slow, enhancing retention and short-distance transport, and minimizing transport out of the
583 GOA. A negative MEI (the Multivariate ENSO index) indicates La Niña conditions (weak
584 circulation) whereas a positive MEI indicates El Niño conditions (strong circulation; Comes and
585 DiLorenzo, 2007). NPI is area-weighted sea level pressure over the region between 30°N and
586 65°N with a positive NPI reflecting a weaker Aleutian Low and slower gyre circulation. During
587 the examined period, Pacific cod recruitment in the GOA was positively correlated with NPI ($r =$
588 0.496 , $p = 0.043$) and negatively associated with the MEI ($r = -0.421$, $p = 0.092$). These patterns
589 basin-scale patterns appear to be associated with climate-related patterns of delivery of Pacific
590 cod larvae to specific nursery regions. For example, settlement in both the West Shumagin area
591 (the nursery area with the greatest fraction of settling fish) and Prince William Sound (important
592 for collection of upstream larvae as well as retention) were positively correlated with the NPI
593 and negatively correlated with the MEI.

594 It is difficult to isolate the specific mechanisms linking regional climate indices to
595 population connectivity and recruitment as aspects of climate and ocean conditions are generally
596 linked. For example, overall recruitment was also negatively correlated ($r = -0.505$, $p = 0.039$)
597 with the PDO, which could suggest a positive effect on cod survival of low temperatures or
598 central GOA wind events (Ladd et al. 2016). However, the PDO was only weakly correlated with
599 settlement in the West Shumagin area and not correlated with settlement in Prince William
600 Sound. The lack of consistent correlations between the PDO and settlement in the model could
601 be due to the focus on transport-related processes in the model. While growth and development
602 of cod early life stages were driven by temperature, other potentially temperature-mediated
603 biological processes such as prey availability and mortality were not incorporated throughout the
604 model. Interestingly, the AO showed virtually no correlation with recruitment or settlement into
605 any specific region.

606 Trust in the results of modelling studies generally requires some degree of validation of
607 the models. The ROMS model is able to reproduce currents and temperature in the GOA (Coyle
608 et al., 2012). Details of the circulation, such as the precise locations of medium- and large-scale
609 eddies at specific times (which may affect dispersal and recruitment of young fish, Parada et al.,
610 2016) cannot be expected to be exact due to the stochastic nature of these flow features.
611 Empirical observations to corroborate the Pacific cod IBM are currently limited. Data on larval
612 distribution exist (Doyle and Mier, 2016), but observations are concentrated in the western GOA.
613 Our model also showed juvenile cod settlement all around the GOA and is generally supported
614 by data from the NOAA Nearshore Fish Atlas (Johnson et al., 2012) showing that juvenile cod
615 were caught in every area surveyed around the coastal GOA.

616 To some degree, this latter pattern of settlement was a result of the uniform egg releases
617 that we used to initialize the model, due to the lack of information about specific spawning
618 locations of Pacific cod in the GOA. Also, our settlement criterion was very simple, i.e.
619 epipelagic juveniles were allowed to settle when they first encountered water depths less than 70
620 m. The decision to settle is undoubtedly much more complex. For example, studies have found
621 young cod in eelgrass beds and other emergent vegetation, and associated with mounds of sea
622 cucumbers. These associations may represent post-settlement habitat selection. It was not
623 possible to include these complex factors, as knowledge of settling behavior, and comprehensive
624 maps of potential habitat such as emergent vegetation are not available. However, a coordinated
625 effort to look at spatial variation in abundance and distribution of juvenile Pacific cod in western
626 GOA nurseries is currently underway (Ben Laurel, pers. comm.), which should provide more
627 detailed information to support examination of specific patterns of connectivity.

628 The success of transport from spawning to nursery areas undoubtedly depends on factors
629 other than physical dispersal and temperature effects, which are the main processes included in
630 this model. Predation mortality was not included and it was also not possible to include more
631 complex processes of feeding or bioenergetics due to the lack of data and rates. In the future, the
632 Pacific cod IBM would be greatly improved with better understanding of spawning locations,
633 settling behavior and habitat, and additional data on the distributions of the early life stages of
634 cod throughout the GOA. Information on spatial variation in prey availability, foraging success,
635 and predation vulnerability of these life stages would further improve the model, and allow
636 integration of the suite of processes influencing population connectivity and recruitment. A
637 clearer understanding of these integrated processes would aid in predicting how the Pacific cod
638 stock in the Gulf of Alaska will respond under varying environmental conditions in the short and

639 long term. However, the results of this study show intriguing potential relationships between
640 patterns of connectivity and large-scale climate indices with recruitment of Pacific cod in the
641 GOA.

642

643 **Acknowledgements**

644

645 We thank the North Pacific Research Board for funding the Modelling Component of the
646 Gulf of Alaska Integrated Ecosystem Research Program (GOAIERP) under award #G84, which
647 supported this research. We would also like to acknowledge support from the EcoFOCI group
648 and the RACE Division at the Alaska Fisheries Science Center. This research is contribution
649 EcoFOCI-0863 to NOAA's Fisheries-Oceanography Coordinated Investigations and PMEL
650 contribution number 4451. This publication was partially funded by the Joint Institute for the
651 Study of the Atmosphere and Ocean (JISAO) under NOAA Cooperative Agreement
652 NA15OAR4320063. This manuscript is NPRB publication number 639, Gulf of Alaska Project
653 publication number 23. The authors would like to thank K. Hedstrom for her effort in the initial
654 development of the ROMS Gulf of Alaska model on which our experiments were based. The
655 findings and conclusions in the paper are those of the authors and do not necessarily represent
656 the views of the National Marine Fisheries Service.

657

658 **References**

659

660 Abookire, A. A., J. T. Duffy-Anderson and C. M. Jump. 2007. Habitat associations and diet of
661 young-of-the-year Pacific cod (*Gadus macrocephalus*) near Kodiak, Alaska. *Mar. Biol.*
662 150, 713-726.

663 Alderdice, D. F. and C. R. Forrester. 1971. Effect of salinity, temperature, and dissolved oxygen
664 on early development of the Pacific cod (*Gadus macrocephalus*). *J. Fish. Res. Bd. Can.*
665 28, 883-902.

666 Aydin, K., S. Gaichas, I. Ortiz, D. Kinzey and N. Friday. 2007. A Comparison of the Bering Sea,
667 Gulf of Alaska, and Aleutian Islands Large Marine Ecosystems Through Food Web
668 Modeling. U.S. Dep. Commer., NOAA Tech. Memo. NMFS-AFSC-178, 298 p.

669 Barbeaux, S., K. Aydin, B. Fissel, K. Holsman, B. Laurel, W. Palsson, K. Shotwell, Q. Yang,
670 and S. Zador. 2018. Assessment of the Pacific cod stock in the Gulf of Alaska. Ch. 2 in
671 Stock Assessment and Fishery Evaluation Report for the Groundfish Resources of the
672 Gulf of Alaska, North Pacific Fishery Management Council, 605 W 4th Avenue, Suite
673 306, Anchorage, AK 99501.

674 Beamer, J. P., D.F Hill, A. Arendt, and G.E. Liston. 2016. High-resolution modeling of the
675 coastal freshwater discharge and glacier mass balance in the Gulf of Alaska watershed.
676 *Water Resource Res.* 52, 3888-3909.

677 Berntsen, J., E. Svendsen, E., and M. Ostrowski. 1996. Validation and sensitivity study of a
678 sigma-coordinate ocean model using SKAGEX dataset. *ICES CM* 1996/C:5.

679 Bond, N. A. and D. E. Harrison. 2000. The Pacific Decadal Oscillation, air-sea interaction and
680 central north Pacific winter atmospheric regimes. *Geophys. Res. Lett.* 27, 731-734.

681 Brodeur, R. D. and W. C. Rugen. 1994. Diel vertical distribution of ichthyoplankton in the
682 northern Gulf of Alaska. Fish. Bull. 9, 223–235.

683 Combes, V. and E. Di Lorenzo. 2007. Intrinsic and forced interannual variability of the Gulf of
684 Alaska mesoscale circulation. Prog. Oceanogr. 75(2), 266-286.
685 doi:10.1016/j.pocean.2007.08.011

686 Cooney, R. T. 1986. The seasonal occurrence of *Neocalanus cristatus*, *Neocalanus plumchrus*,
687 and *Eucalanus bungii* over the shelf of the northern Gulf of Alaska. Continental Shelf
688 Res. 5, 541-553.

689 Cooper, D. W., J. T. Duffy-Anderson, W. T. Stockhausen and W. Cheng. 2013. Modeled
690 connectivity between northern rock sole (*Lepidopsetta polyxystra*) spawning and nursery
691 areas in the eastern Bering Sea. J. Sea Res.84, 2-12.

692 Cowen, R. K., C. B. Paris, A. Srinivasan. 2006. Scaling of connectivity in marine populations.
693 Science 311, 522-527.

694 Cowen, R. K., G. Gawarkiewicz, J. Pineda, S. R. Thorrold, F. E. Werner. 2007. Connectivity in
695 Marine Systems: An Overview. Oceanography, 20, 14-21.

696 Coyle, K., W. Cheng, S. Hinckley, E. J. Lessard, T. Whitledge, A.J. Hermann and K. Hedstrom.
697 2012. Model and field observations of effects of circulation on the timing and magnitude
698 of nitrate utilization and production on the northern Gulf of Alaska shelf. Prog. Oceanogr.
699 103, 16-41, doi:10.1016/j.pocean.2012.03.002.

700 Coyle, K. O., A.J. Hermann, and R.R. Hopcroft. *in press (this volume)*. Modeled spatial-temporal
701 distribution of productivity, chlorophyll, iron and nitrate on the northern Gulf of Alaska
702 shelf relative to field observations. Deep Sea Res. II.

703 Coyle, K. O., G. A. Gibson, K. Hedstrom, A. J. Hermann, and R. R. Hopcroft. 2013.
704 Zooplankton biomass, advection and production on the northern Gulf of Alaska shelf
705 from simulations and field observations. *J. Mar. Syst.* 128, 185-207,
706 doi:10.1016/j.jmarsys.2013.04.018.

707 Cunningham, K. M., M. F. Canino, I. B. Spies, and L. Hauser. 2008. Genetic isolation by
708 distance and localized fjord population structure in Pacific cod (*Gadus macrocephalus*):
709 limited effective dispersal in the northeastern Pacific Ocean. *Can. J. Fish. Aquat. Sci.* 66,
710 153-166.

711 Dai, A., T. Qian, K. E. Trenberth, and J. D. Milliman. 2009. Changes in continental freshwater
712 discharge from 1948-2004. *J. Climate* 22, 2773-2791.

713 Danielson, S., E. Curchitser, K. Hedstrom, T. Weingartner, P. Stabeno. 2011. On ocean and sea
714 ice modes of variability in the Bering Sea. *J. Geophys. Res.* 116, C12034,
715 doi:10.1029/2011JC007389.

716 Dean, T. A., L. Haldorson, D. R. Laur, S. C. Jewett and A. Blanchard. 2000. The distribution of
717 nearshore fishes in kelp and eelgrass communities in Prince William Sound, Alaska:
718 associations with vegetation and physical habitat characteristics. *Environ. Biol. Fishes* 57,
719 271-287.

720 Di Lorenzo, E. and N. Mantua. 2016. Multi-year persistence of the 2014/2015 North Pacific
721 marine heatwave. *Nature Climate Change* 6, 1042-1048.

722 Dobbins, E. L., A. J. Hermann, P. Stabeno, N. A. Bond and R. C. Steed. 2009. Modeled transport
723 of freshwater from a line-source in the coastal Gulf of Alaska. *Deep-Sea Res. II* 56, 2409.
724 doi:10.1016/j.dsr2.2009.02.004.

725 Doyle, M. J., and K. L. Mier. 2016. Early life history pelagic exposure profiles of selected
726 commercially important fish species in the Gulf of Alaska. *Deep-Sea Res. II*, 132, 162-
727 193.

728 Dunn, J. R. and A. C. Matarese. 1987. A review of the early life history of northeast Pacific
729 gadoid fishes. *Fish. Res.* 5, 163-184.

730 Gibson, G. A., W. Stockhausen, K.O. Coyle, S. Hinckley, C. Parada, A. Hermann, M. Doyle, C.
731 Ladd. *In press*. An individual-based model for Sablefish: Exploring the connectivity
732 between potential spawning and nursery grounds in the Gulf of Alaska. *Deep-Sea Res. II*.

733 Haidvogel, D. B., H. Arango, W. P. Budgell, B. D. Cornuelle, E. Curchitser, E. Di Lorenzo, K.
734 Fennel, W. R. Geyer, A. J. Hermann, L. Lanerolle, J. Levin, J. C. McWilliams, A. J.
735 Miller, A. M. Moore, T. M. Powell, A. F. Shchepetkin, C. R. Sherwood, R. P. Signell, J.
736 C. Warner, J. Wilkin. 2008. Regional Ocean Forecasting in Terrain-following
737 Coordinates: Model Formulation and Skill Assessment. *J. Comput. Phys.* 227, 3595-
738 3624.

739 Hermann, A. J., E. N. Curchitser, D. B. Haidvogel and E. L. Dobbins. 2009a. A comparison of
740 remote versus local influence of El Nino on the coastal circulation of the Northeast
741 Pacific. *Deep-Sea Res. II* 56, 2427-2443. doi:10.1016/j.dsr2.2009.02.005.

742 Hermann, A. J., S. Hinckley, E. L. Dobbins, D. B. Haidvogel, N. A. Bond, C. Mordy, N. Kachel
743 and P. J. Stabeno. 2009b. Quantifying cross-shelf and vertical nutrient flux in the Gulf of
744 Alaska with a spatially nested, coupled biophysical model. *Deep-Sea Res. II*, 56, 2474-
745 2486, doi:10.1016/j.dsr2.2009.02.008.

746 Higgins, R.W., Y. Zhou and H.-K. Kim. 2001. Relationships between El Niño-Southern
747 Oscillation and the Arctic Oscillation: A Climate-Weather Link. *NCEP/Climate*

748 Prediction Center ATLAS 8.
749 http://www.cpc.ncep.noaa.gov/research_papers/ncep_cpc_atlas/8/index.html

750 Higgins, R.W., A. Leetmaa, and V. E. Kousky. 2002. Relationships between climate variability
751 and winter temperature extremes in the United States. *J. Climate* 15, 1555-1572.

752 Hill, D. F., N. Bruhis, S.E. Calos, A. Arendt, and J. Beamer, J., 2015. Spatial and temporal
753 variability of freshwater discharge into the Gulf of Alaska. *J. Geophys. Res. Oceans*. 120,
754 634-646.

755 Hinckley, S., A. J. Hermann and B. A. Megrey. 1996. Development of a spatially-explicit,
756 individual-based model of marine fish early life history. *Mar. Ecol. Prog. Ser.* 139, 47-68.

757 Hinckley, S., A. J. Hermann, K. L. Mier, and B. A. Megrey. 2001. Importance of spawning
758 location and timing to successful transport to nursery areas: a simulation study of Gulf of
759 Alaska walleye pollock. *ICES J. of Mar. Sci.* 58, 1042–1052.

760 Hinckley, S., K. O. Coyle, G. Gibson, A. J. Hermann, and E. L. Dobbins. 2009. A biophysical
761 NPZ model with iron for the Gulf of Alaska: Reproducing the differences between an
762 oceanic HNLC ecosystem and a classical northern temperate shelf ecosystem. *Deep-Sea*
763 *Res. II* 56, 2520-2536. doi:10.1016/j.dsr2.2009.03.003.

764 Hinckley, S., C. Parada, J. K. Horne, M. Mazur and M. Woillez. 2016. Comparison of
765 individual-based model output to data using a model of walleye pollock early life history
766 in the Gulf of Alaska. *Deep-Sea Res. II* 132, 240-262.

767 Hinrichsen, H-H., J. O. Schmidt, C. Petereit, C. Mölmann. 2005. Survival probability of Baltic
768 larval cod in relation to spatial overlap patterns with its prey obtained from drift model
769 studies. *ICES J. of Mar. Sci.*, 62, 878-885.

770 Hirschberger, W. A. and G. B. Smith. 1983. Spawning of twelve groundfish species in the
771 Alaska and Pacific Coast regions, 1975-81. U.S. Dep. Commer., NOAA Tech. Memo.
772 NMFS F/NWC-44, 50 pp.

773 Hjort, J. 1914. Fluctuations in the great fisheries of northern Europe, viewed in the light of
774 biological research. Rapports et Procès-Verbaux des Réunions du Conseil Permanent
775 International pour l'Exploration de la Mer, 20, 1–228.

776 Houde, D.E. 2009. Recruitment variability. *in* T. Jakobsen, M. J. Fogarty, B. A. Megrey and E.
777 Moksness, *Fish Reproductive Biology*, Chapter 3, Wiley-Blackwell. ISBN 978-1-4051-
778 2126-2.

779 Hurst, T. P., D. W. Cooper, J. S. Scheingross, E. M. Seale, B. J. Laurel and M. L. Spencer. 2009.
780 Effects of ontogeny, temperature, and light on vertical movements of larval Pacific cod
781 (*Gadus macrocephalus*). *Fish. Oceanogr.* 18, 301-311.

782 Hurst, T. P., B. J. Laurel, L. Cianelli. 2010. Ontogenetic patterns and temperature-dependent
783 growth rates in early life stages of Pacific cod (*Gadus macrocephalus*). *Fish. Bull.* 108,
784 382–392.

785 Janout, M. A., T. J. Weingartner, S. R. Okkonen, T. E. Whitley, D. L. Musgrave. 2009. Some
786 characteristics of Yakutat Eddies propagating along the continental slope of the northern
787 Gulf of Alaska. *Deep-Sea Res. II* 56, 2444-2459.

788 Johnson, S. W., A. D. Neff, J. F. Thedinga, M. R. Lindeberg, and J. M. Maselko. 2012. Atlas of
789 nearshore fishes of Alaska: A synthesis of marine surveys from 1998 to 2011. U.S. Dep.
790 Commer., NOAA Tech. Memo. NMFS-AFSC-239, 261 p.

791 Kim, J. J., W. Stockhausen, S. Kim, Y-K. Cho, G-H. Seo, J-S. Lee. 2015. Understanding
792 interannual variability in the distribution of, and transport processes affecting, the early

793 life stages of *Todarodes pacificus* using behavioral-hydrodynamic modeling approaches.
794 Prog. Oceanogr. 138, 571-583. doi: <http://dx.doi.org/10.1016/j.pocean.2015.04.003>.

795 Ladd, C. A., and P. J. Stabeno. 2009. Freshwater transport from the Pacific to the Bering Sea
796 through Amukta Pass. Geophys. Res. Lett., 36, L14608, doi:10.1029/2009GL039095.

797 Ladd, C. A., N. B. Kachel, C. W. Mordy and P. J. Stabeno. 2005. Observations from a Yakutat
798 eddy in the northern Gulf of Alaska. J. Geophys. Res., 110, C03003, doi:
799 10.1029/2004JC002710.

800 Large, W. G., S. G. Yeager, 2008. The global climatology of an interannually varying air-sea
801 flux data set. Clim. Dyn. 33, 341-364.

802 Large, W. G., J. C. McWilliams, S. C. Doney, 1994. Oceanic vertical mixing: a review and a
803 model with a nonlocal boundary layer parameterization. Rev. Geophys. 32, 363-403.

804 Laur, D. and L. Haldorson. 1996. Coastal habitat studies: the effect of the Exxon Valdez oil spill
805 on shallow subtidal fishes in Prince William Sound. In: Rice, S.D., R.B. Spies, D.A.
806 Wolfe and B.A. Wright (eds) American Fisheries Society Symposium 18: Proceedings of
807 the Exxon Valdez oil spill symposium. American Fisheries Society, Bethesda, Maryland,
808 pp. 659-670.

809 Laurel, B. J., R. S. Gregory and J. A. Brown. 2003. Settlement and distribution of age-0 juvenile
810 cod *Gadus morhua* and *G. ogac*, following a large-scale habitat manipulation. Mar. Ecol.
811 Prog. Ser. 262, 241-252.

812 Laurel, B. J., A. W. Stoner, C. H. Ryer, T. P. Hurst, A. A. Abookire, 2007. Comparative habitat
813 associations in juvenile Pacific cod and other gadids using seines, baited cameras and
814 laboratory techniques. J. Exp. Mar. Biol. Ecol. 351, 42-55.

815 Laurel, B. J., T. P. Hurst, L. A. Copeman and M. W. Davis. 2008. The role of temperature on the
816 growth and survival of early and late hatching Pacific cod larvae (*Gadus macrocephalus*).
817 J. Plankton Res. 30(9), 1051-1060.

818 Laurel, B. J., C. H. Ryer, B. Knoth , and A. W. Stoner. 2009. Temporal and ontogenetic shifts in
819 habitat use of juvenile Pacific cod (*Gadus macrocephalus*). J. Exp. Mar. Biol. Ecol. 377,
820 28–35.

821 Lett, C., P. Verley, C. Mullon, C. Parada, T. Brochier, P. Penven and B. Blake. 2008. A
822 Lagrangian tool for modeling ichthyoplankton dynamics. Environ. Modelling Software
823 23, 1210-1214.

824 Mantua, N. J., S. R. Hare, Y. Zhang, J. M. Wallace, and R. C. Francis.1997. A Pacific
825 interdecadal climate oscillation with impacts on salmon production. Bull. Am. Met. Soc.
826 78, 1069-1079.

827 Marchesiello, P., J. C. McWilliams, and A. F. Shchepetkin. 2001. Open boundary conditions for
828 long-term integration of regional oceanic models. Ocean Modelling 3, 1-20.

829 Matarese, A.C., A. W. Kendall, D. M. Blood, and B. M. Vinter. 1989. Laboratory Guide to Early
830 Life Stages of Northeast Pacific Fishes. NOAA Technical Report NMFS 80. 652 pp.

831 Mecklenburg, C. W., T. A. Mecklenburg, and L. K. Thorsteinson. 2002. Fishes of Alaska.
832 American Fisheries Society, Bethesda, Md., 1037 pp.

833 Megrey, B. A. and S. Hinckley. 2001. The effect of turbulence on feeding of larval fishes: a
834 sensitivity analysis using an individual-based model. ICES J. Mar. Sci. 58(5), 1015-1029.

835 Narimatsu, Y., T. Hattori, Y. Ueda, H. Matsuzaka, M. Shiogaki, 2007. Somatic growth and
836 otolith microstructure of larval and juvenile Pacific cod *Gadus macrocephalus*. Fish. Sci.
837 73(6), 1257-1264.

838 North, E. W., A. Gallego and P. Petitgas. 2009. Manual of recommended practices for modelling
839 physical-biological interactions during fish early life. ICES Coop. Res. Rep. No. 295.

840 Okkonen, S. R. T.J. Weingartner, S.L. Danielson, D.L. Musgrave, and G.M. Schmidt. 2003.
841 Satellite and hydrographic observations of eddy-induced shelf-slope exchange in the
842 northwestern Gulf of Alaska. *J. of Geophysical Res.* 108 (c2), 3033.
843 doi 10.1029/2002JC001342.

844 Ottmar, M. L. and T. P. Hurst. 2012. Thermal effects on swimming activity and habitat choice in
845 juvenile Pacific cod (*Gadus macrocephalus*). *Mar. Biol.* 159, 2185-2194. doi
846 10.1007/s00227-012-2004-8.

847 Parada, C., D. A. Armstrong, B. Ernst, S. Hinckley, and J. M. (Lobo) Orensanz. 2010. Spatial
848 dynamics of snow crab (*Chionoecetes opilio*) in the eastern Bering Sea—putting together
849 the pieces of the puzzle. *Bull. Mar. Sci.* 86 (2), 413-437.

850 Parada, C., S. Hinckley, J. Horne, M. Mazur, A. Hermann, E. Curchister. 2016. Modeling
851 connectivity of walleye pollock in the Gulf of Alaska: Are there any linkages to the
852 Bering Sea and Aleutian Islands? *Deep-Sea Res. II* 132, 227-239.

853 Paris, C. B., K. C. Lindeman, R. Claro, J. L. Fortuna, R. K. Cowen, R. K. 2004. Modeling larval
854 transport from snapper (Lutjanidae) spawning aggregations in Cuba. *Proc. Gulf and*
855 *Caribbean Fish. Inst.* 55, 570-576.

856 Pelc, R. A., R. R. Warner, S. D. Gaines, C. B. Paris. 2010. Detecting larval export from marine
857 reserves. *Proc. Nat. Acad. Sci. USA* 107(43), 18266-18271.

858 Reed, R. K., and J. D. Schumacher. 1984. Additional current measurements in the Alaskan
859 Stream near Kodiak Island. *J. Phys. Oceanogr.* 14(7), 1,239-1,246.

860 Richwine, K. A., K. R. Smith, and R. A. McConnaughey. 2018. Surficial sediments of the
861 eastern Bering Sea continental shelf: EBSSSED-2 database documentation. U.S. Dep.
862 Commer., NOAA Tech. Memo. NMFS-AFSC-377, 48 p.

863 Royer, T. C. 1982. Coastal freshwater discharge in the northeast Pacific. J. Geophys. Res.
864 87(C3), 2017-2021.

865 Royer, T. 1998. Coastal Processes in the Northern North Pacific. John Wiley & Sons, Inc., 605
866 Third Ave. New York NY 10158 USA.

867 Rugen, W. C., and A. C. Matarese. 1988. Spatial and temporal distribution and relative
868 abundance of Pacific cod (*Gadus macrocephalus*) larvae in the western Gulf of Alaska.
869 NWAFC Processed Report 88-18, NOAA/NMFS, Seattle, Washington, 53 pp.

870 Saha, S. and coauthors. 2010. The NCEP Climate Forecast System Reanalysis. Bull. Amer.
871 Meteor. Soc. 91, 1015.1057. doi: 10.1175/2010BAMS3001.1

872 Shchepetkin, A. F., J. C. McWilliams. 2005. The regional oceanic modeling system (ROMS): a
873 split-explicit, free-surface, topography-following-coordinate oceanic model, Ocean
874 Modelling 9 (4), 347-404.

875 Smith, G. B., G. E. Walters, P. A. Raymore and W. A. Hirschberger. 1984. Studies of the
876 distribution and abundance of juvenile groundfish in the northwestern Gulf of Alaska,
877 1980-1982: Part I. Three-year comparisons. NOAA Tech. Mem. NMFS-F/NWC-59.

878 Sjøiland, H., and M. D. Skogen. 2000. Validation of a three-dimensional biophysical model using
879 nutrient observations in the North Sea. ICES J. Mar. Sci. 57, 816–823.

880 Stabeno, P. J., R. K. Reed, and J. D. Schumacher. 1995. The Alaska Coastal Current: Continuity
881 of transport and forcing. J. Geophys. Res. 100 (C2), 2477-2485.

882 Stabeno, P. J., N. A. Bond, A. J. Hermann, N. B. Kachel, C. W. Mordy and J. E. Overland. 2004.
883 Meteorology and oceanography of the northern Gulf of Alaska. *Cont. Shelf Res.* 24 (7-8),
884 859–897.

885 Stabeno, P.J., S. Bell, W. Cheng, S. Danielson, N.B. Kachel, and C.W. Mordy. 2016.

886 Stachura, M. M., T. E. Essington, N. J. Mantua, A. B. Hollowed, M. A. Haltuch, P. D. Spencer,
887 T. A. Branch and M. J. Doyle. 2014. Linking Northeast Pacific recruitment synchrony to
888 environmental variability. *Fish. Oceanogr.* 23 (5), 389-408. Long-term observations of
889 Alaska Coastal Current in the northern Gulf of Alaska. *Deep-Sea Res. II*
890 doi:10.1016/j.dsr2.2015.12.016

891 Stark, J. W. 2007. Geographic and seasonal variations in maturation and growth of female
892 Pacific cod (*Gadus macrocephalus*) in the Gulf of Alaska and Bering Sea. *Fish. Bull.*
893 105, 396–407.

894 Stockhausen, W., R. Lipcius and B. Hickey. 2000. Joint effects of larval dispersal, population
895 regulation, marine reserve design and exploitation on production and recruitment in the
896 Caribbean spiny lobster. *Bull. Mar. Sci.* 66 (3), 957-990.

897 Stockhausen, W. and R. Lipcius. 2001. Single large or several small marine reserves for the
898 Caribbean spiny lobster? *Mar. Freshwater Res.* 50, 1605-1614.

899 Stockhausen, W. and R. Lipcius. 2003. Simulated effects of seagrass loss and restoration on
900 settlement and recruitment of blue crab postlarvae and juveniles in the York River,
901 Chesapeake Bay. *Bull. Mar. Sci.* 72, 409-422.

902 Stockhausen, W. and A. Hermann. 2007. Modeling larval dispersion of rockfish: A tool for
903 marine reserve design? In: J. Heifetz, J. DiCosimo, A.J. Gharrett, M.S. Love, T.

904 O'Connell, and R. Stanley (eds.), Biology, assessment, and management of North Pacific
905 rockfishes. Alaska Sea Grant College Program, University of Alaska Fairbanks.

906 Stockhausen, W. T., K. O. Coyle, A. J. Hermann, D. Blood, M. Doyle, G. Gibson, S. Hinckley,
907 C. Ladd, C. Parada. *In press*. Running the Gauntlet: Connectivity between natal and
908 nursery areas for arrowtooth flounder (*Atheresthes stomias*) in the Gulf of Alaska, as
909 inferred from a biophysical Individual-based Model. Deep-Sea Res. II.

910 Stockhausen, W. T., K. O. Coyle, A. J. Hermann, M. Doyle, , G. Gibson, S. Hinckley, C. Ladd,
911 C. Parada. *In press*. Running the Gauntlet: Connectivity between natal and nursery areas
912 for Pacific ocean perch (*Sebastes alutus*) in the Gulf of Alaska, as inferred from a
913 biophysical Individual-based Model. Deep-Sea Res. II.

914 Thomson, J.A. 1963. On the demersal quality of fertilized eggs of Pacific cod, *Gadus*
915 *macrocephalus* Tilesius. J. Fish. Res. Board Can. 20, 1087–1088.

916 Trenberth, K. E. and J. W. Hurrell. 1994. Decadal atmosphere-ocean variations in the Pacific
917 Climate Dynamics 9, 303-319

918 Trenberth, K. E., and J. W. Hurrell, 1995: Decadal climate variations in the Pacific. National
919 Research Council, Natural Climate Variability on Decade-to-Century Time Scales. D. G.
920 Martinson, K. Bryan, M. Ghil, M. M. Hall, T. R. Karl, E. S. Sarachik, S. Sorooshian, and
921 L. D. Talley, Eds., National Academy Press, Washington, D.C. pp. 472-481.

922 Vaz, R. A. N. and J.H. Simpson. 1994. Turbulence closure modeling of estuarine stratification. J.
923 Geophys. Res. Oceans 99, 16143-16160.

924 Werner F. E., J. A. Quinlan, R. G. Lough, D.R. Lynch. 2001. Spatially-explicit individual based
925 modeling of marine populations: a review of the advances in the 1990s. Sarsia 86, 411-
926 421.

927 Wolter, K., and M. S. Timlin. 1993. Monitoring ENSO in COADS with a seasonally adjusted
928 principal component index. Proc. of the 17th Climate Diagnostics Workshop, Norman,
929 OK, NOAA/NMC/CAC, NSSL, Oklahoma Clim. Survey, CIMMS and the School of
930 Meteor., Univ. of Oklahoma. pp. 52-57. <http://www.esrl.noaa.gov/psd/enso/mei/WT1.pdf>

931 Wolter, K., and M. S. Timlin. 2011. El Niño/Southern Oscillation behaviour since 1871 as
932 diagnosed in an extended multivariate ENSO index (MEI.ext). *Intl. J. Climatology* 31,
933 1074-1087.

934 Zhang, Y., J. M. Wallace and D. S. Battisti, 1997. ENSO-like interdecadal variability: 1900-93.
935 *J. Climate*. 10, 1004-1020.

936

937

938 Table 1. Parameter values, equations and algorithms for Pacific cod IBM.

939

940

Param	Description	Value	Equation/Comments	Units	Source
Egg Stage					
g_E	Growth rate		$g_E = 0.104 + 0.024T - 0.00002T^2$ where, T = temperature (°C)	mm d ⁻¹	Hurst et al., 2010
z_{minE}	Min spawning depth	20		m	Dunn and Matarese 1987
z_{maxE}	Max spawning depth	200		m	Dunn and Matarese 1987
v_E	Egg ascent rate	0	Attached to bottom	ms ⁻¹	Thomson 1963, Alderdice and Forrester, 1971, Dunn and Matarese 1987
d_{minE}	Min stage duration	8		days	
sd_E	Actual Stage duration		$sd_E = 46.597 - 4.079T$ where, T = temperature (°C)	days	B. Laurel, NOAA/AFSC pers. comm.
sr_E	Egg stage ratio		$sr_E = sr_E + \left(\frac{1.0}{sd_E}\right) dt$ where, dt =time step		Trigger for transition to

					next stage ($sr_E \geq 1$)
Yolk-sac Larval Stage					
g_Y	Growth rate		$g_Y = 0.0179 + 0.015T - 0.0001T^2$ where, T=temperature (°C)	mm d ⁻¹	Hurst et al., 2010
z_{minY}	Min depth	0		m	Brodeur and Rugen, 1994
z_{maxY}	Max depth	40		m	Brodeur and Rugen, 1994
v_Y	Vertical velocity	1×10^{-4}		ms ⁻¹	Random up/down
d_{minY}	Min stage duration	2		days	
d_{maxY}	Max stage duration	15		days	
PNR	Point of no return		$PNR = 34.67e^{-0.126T}$ where, T = temperature (°C)	days	Laurel et al., 2008
yd	Days to yolk- sac absorption		$yd = 14.7662e^{-0.235T}$ where, T = temperature (°C)	days	Laurel et al., 2008
sr_Y	Yolk-sac stage ratio		$sr_Y = sr_Y + \left(\frac{1.0}{yd}\right) dt$ where, dt=time step		
p	Probability of feeding		$p = p + \left(\frac{1.0}{PNR - yd}\right) d$		
Pre-flexion Feeding Larval Stage					
g_F	Growth rate		$g_F = 0.0179 + 0.015T - 0.0001T^2$ Where T = temperature (°C)	mm d ⁻¹	Hurst et al. (2010)

z_{minF}	Min. depth	0		m	Brodeur and Rugen, 1994
z_{maxF}	Max depth	40		m	Brodeur and Rugen, 1994
T_F	Standard Length (SL) to Total Length (TL) conversion		$TL = SL + \frac{0.5169}{0.9315}$	mm	B. Laurel, NOAA/AFSC pers. comm.
v_F	Vertical velocity		$v_F = ((0.081221 + 0.043168 * \log_{10}T)TL^{1.49652})/1000.0$ where, T = temperature (°C)	ms ⁻¹	T. Hurst, NOAA/AFSC pers. comm.
d_{minF}	Min stage duration	5		days	
f_F	Length at flexion	13.5		mm	Matarese et al., 1989
Tr_F	Stage transition		$Length > f_F$	mm	
Post-flexion Feeding Larval Stage					
g_{PF}	Growth rate		$g_{PF} = 0.034 + 0.043T - 0.0008T^2$ where, T = temperature (°C)	mm d ⁻¹	Hurst et al., 2010
L_{maxPF}	Length at transformation	25		mm	Dunn and Matarese, 1987
$z_{d_{minPF}}$	Min daytime	20			Hurst et al., 2009

	depth				
$z_{d_{maxPF}}$	Max daytime depth	40		m	Hurst et al., 2009
$z_{N_{minPF}}$	Min nighttime depth	0		m	Hurst et al., 2009
$z_{N_{maxPF}}$	Max nighttime depth	20		m	Hurst et al., 2009
T_{PF}	Standard Length (SL) to Total Length (TL) conversion		$TL = SL + \frac{0.5169}{0.9315}$	mm	B. Laurel, NOAA/AFSC pers. comm.
v_{PF}	Vertical velocity		$v_{PF} = ((0.081221 + 0.043168 * \log_{10}T)TL^{1.49652})/1000.0$ where, T = temperature (°C)	ms ⁻¹	T. Hurst, NOAA/AFSC pers. comm.
Tr_{PF}	Stage transition	Tr_Y	$Length > L_{maxPF}$	mm	
Epipelagic Juvenile Stage					
g_E	Growth rate		$g_E = -0.081 + 0.079T - 0.003T^2$ where, T = temperature (°C)	mm d ⁻¹	Hurst et al., 2010
$z_{d_{minE}}$	Min daytime depth	20		m	Hurst et al., 2009

$z_{d_{maxE}}$	Max daytime depth	40		m	Hurst et al., 2009
$z_{N_{minE}}$	Min nighttime depth	0		m	Hurst et al., 2009
$z_{N_{maxE}}$	Max nighttime depth	20		m	Hurst et al., 2009
v_E	Vertical velocity		$v_E = ((0.081221 + 0.043168 * \log_{10}T)TL^{1.49652})/1000.0$ where, $T =$ temperature ($^{\circ}C$)	ms ⁻¹	T. Hurst, NOAA/AFSC pers. comm.
h_{minE}	Min settlement depth	10		m	Smith et al., 1984
h_{maxE}	Max settlement depth	70		m	Smith et al., 1984
Tr_E	Stage transition	Tr_Y	$Depth \geq h_{min}$ and $Depth \leq h_{max}$	m	
Benthic Juvenile Stage					
g_J	Growth rate		$g_E = -0.081 + 0.079T - 0.003T^2$ where, $T =$ temperature ($^{\circ}C$)	mm d ⁻¹	Hurst et al., 2010
h_{minJ}	Min depth	10		m	Minimum model depth
h_{maxJ}	Max depth	70			Smith et al., 1984

942

943

Table 2. Results of grid size test.

Grid Size (km)	Number of Matching Settlement Zones in	
	Top 10	Number Simulated
1	n/a	5563
2.5	10	906951
5	9	221952
7	9	101953
10	8	64 954
		955

959 Table 3. Correlations coefficients between the time series (1996-2011) of percent settled in each
 960 nursery area and overall percent settled from the Pacific cod IBM, recruitment (Rct: ln-
 961 transformed estimated basin-wide age-0 recruitment) and physical indices. ** indicates
 962 correlations that are significant at $p < 0.05$; * indicates correlations that are significant at $p <$
 963 0.10 are italicized. P-values are not corrected for multiple comparisons.

Nursery					
Area	Rct	MEI	PDO	NPI	AO
101	-0.612**	0.021	0.096	-0.389	0.178
102	0.063	-0.121	-0.475*	0.199	0.194
103	-0.275	0.440*	0.205	-0.213	-0.008
104	0.353	0.104	-0.201	0.201	-0.339
105	0.706**	-0.348	-0.491**	0.419*	0.035
106	0.049	-0.462*	-0.302	0.480*	0.227
107	-0.703**	0.092	0.350	-0.310	0.131
108	-0.581**	0.028	0.186	-0.149	0.254
109	-0.146	-0.005	0.387	-0.394	-0.039
110	-0.379	-0.061	0.289	-0.442*	-0.056
111	0.412	-0.308	-0.244	0.317	-0.269
112	0.275	-0.535**	-0.429*	0.531**	-0.023
113	0.180	0.129	0.330	-0.412	-0.111
TotFracSettle	-0.099	-0.438*	-0.122	0.178	0.070
d					

966 List of Figures

967 Fig. 1. Time series of female spawning stock biomass (SSB) and age-0 recruitment (Barbeaux et
968 al., 2018) for Gulf of Alaska Pacific cod.

969 Fig. 2. The Gulf of Alaska, with connectivity zones used in Pacific cod IBM. Spawning zones
970 are < 70 m (102 – 113) and 70 to 200 m (202 – 213). Nursery areas are < 70 m (numbered 101-
971 113). Offshore zones start at the 200 m isobaths and extends 125-150 km offshore from that
972 isobaths (numbered 1-13). The Deep Ocean zone is number 0. Alongshore zone names are
973 indicated. The box around the plot indicates the extent of the 3-km ROMS grid.

974 Fig. 3. Conceptual model of the early life history of Pacific cod, showing movement across the
975 shelf from spawning to settlement. X-axis represents time; t_0 is the spawning date. The y-axis
976 represents depth. Numbers above 0-depth line represent individual size.

977 Fig. 4. Average connectivity for the Pacific cod IBM simulation years (1997-2013). The y-axis
978 of both panels shows the spawning areas, with 102-113 representing the shallow (<70 m)
979 spawning areas, and 202-213 representing the deep (70–200 m) spawning areas. Sink area 998
980 representing individuals that left the 3-km grid (mostly to the southwest along the Alaska
981 Peninsula) is shown in a separate panel due to a difference in scale. The x-axis of the matrix
982 shows the sink areas: 101–113 are nursery areas (<70 m), 201–213 are regions where the depth is
983 70–200 m, 1–12 are from the 200 m isobaths to approximately 150 km offshore. Area 0 is the
984 GOA deep basin. The shading represents the probability of moving from spawning area to
985 ending area. Heavy lines on the matrix delineate the different depth regions.

986 Fig. 5. Standard deviation of connectivity for the Pacific cod IBM simulation years (1997-2013).
987 The y-axis shows the spawning areas, with 102-113 representing the shallow (<70 m) spawning
988 areas, and 202-213 representing the deep (70–200m) spawning areas. The x-axis of the matrix

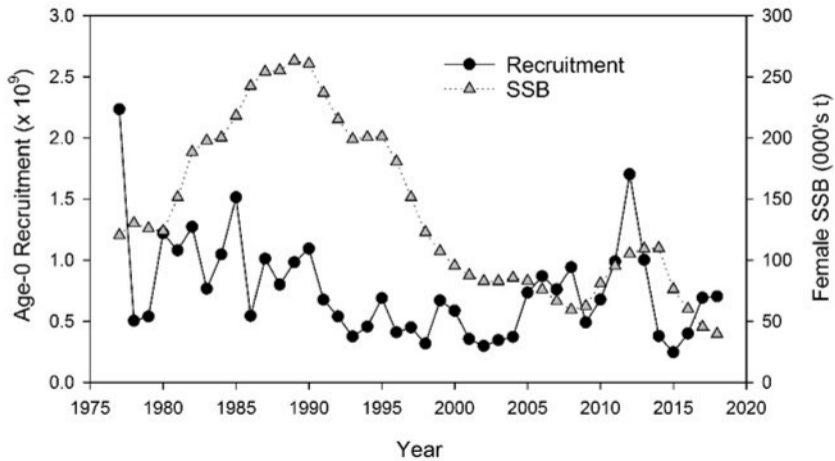
989 shows the sink areas: 101–113 are nursery areas (<70 m), 201–213 are regions where the depth is
990 70–200 m, 1–12 are from the 200 m isobaths to approximately 150 km offshore. Area 0 is the
991 GOA deep basin. Sink area 998 represents individuals that left the 3-km grid, mostly to the
992 southwest along the Alaska Peninsula. The shading represents the standard deviation. Heavy
993 lines on the matrix delineate the different depth regions.

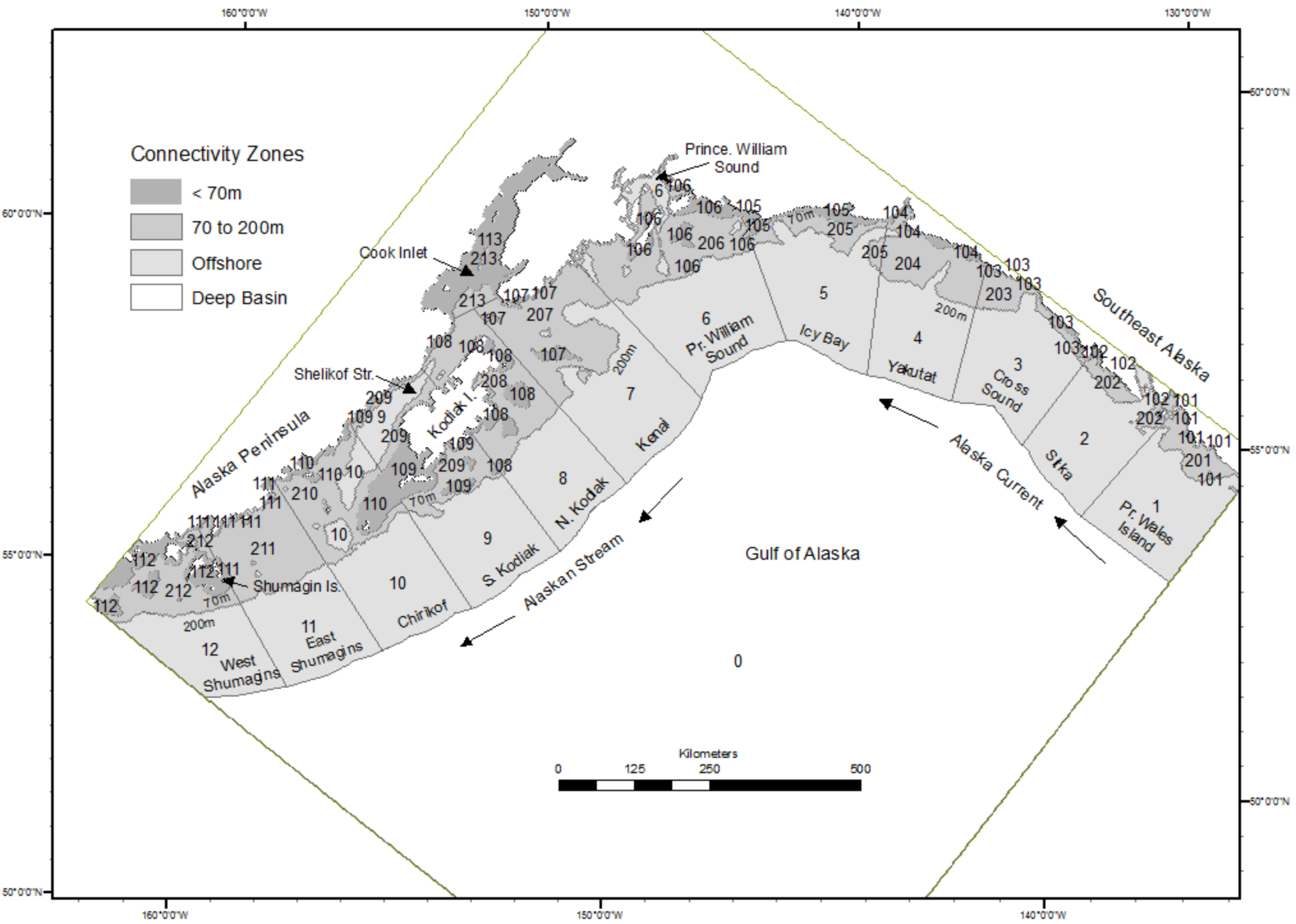
994 Fig. 6. Spawning areas for selected nursery or ending (Z998) regions. Each panel represents one
995 nursery or ending area. The x-axis shows the spawning areas, with 102-112 being the shallow
996 (<70 m) spawning areas, and 202-212 being the deep (70–200 m) spawning areas. The y-axis
997 represents the probability of transport from each spawning area to the nursery or ending area
998 represented in the panel.

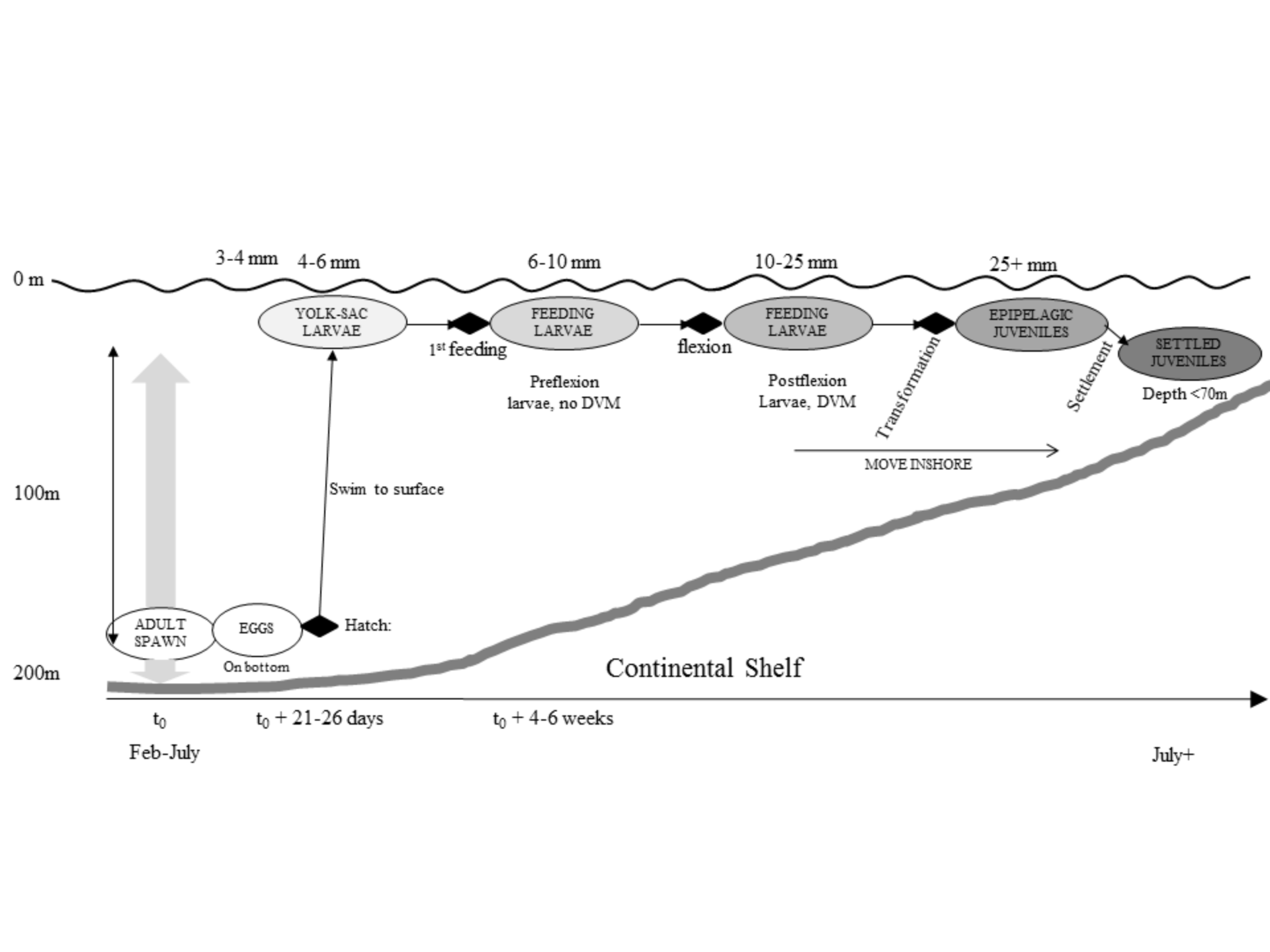
999 Fig. 7. Time series of *NDI* and *OC*, indices calculated from the Pacific cod IBM connectivity
1000 matrices.

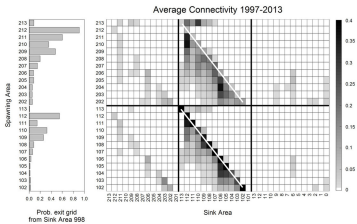
1001 Fig. 8. Matrix showing the difference in connectivity probabilities between 1998, the year with
1002 the highest *NDI*, and the average connectivity matrix from the 1997-2013 time series. The y-axis
1003 shows the spawning areas, with 102-113 representing the shallow (<70 m) spawning areas, and
1004 202-213 representing the deep (70–200 m) spawning areas. The x-axis of the matrix shows the
1005 sink areas. Areas 101–113 are the nursery areas (<70 m), areas 201–213 are regions where the
1006 depth is 70–200 m. Area 998 indicates the probabilities of exiting the 3-km grid from all
1007 spawning areas. Areas 1 – 12 are from the 200 m isobaths to approximately 150 km offshore.
1008 Sink area 0 is the GOA deep basin and sink area 998 represents individuals that left the 3-km
1009 grid. The shading represents the difference in probability of transport from spawning area to
1010 ending area.

1011 Fig. 9. A. Fraction settled (of all individuals simulated) in each nursery area. B. Fraction settled
1012 of individuals from the shallow spawning areas. C. Fraction settled of individuals from the deep
1013 spawning areas. D. Fraction settled (of all individuals simulated) for each year of the simulation.
1014

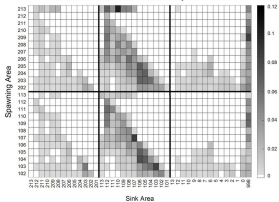


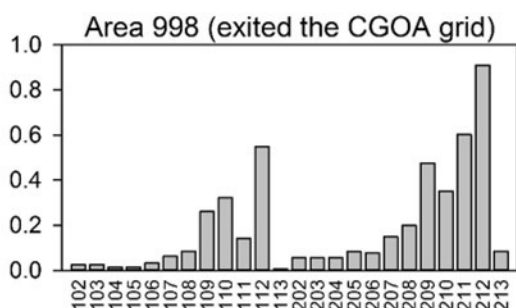
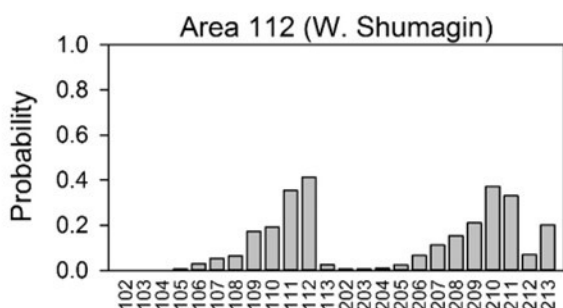
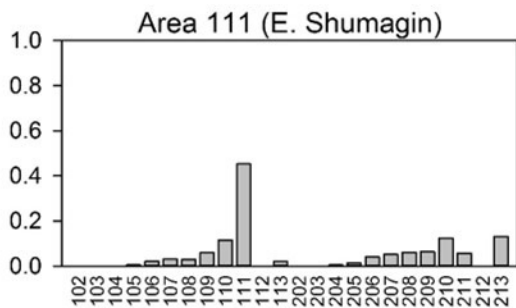
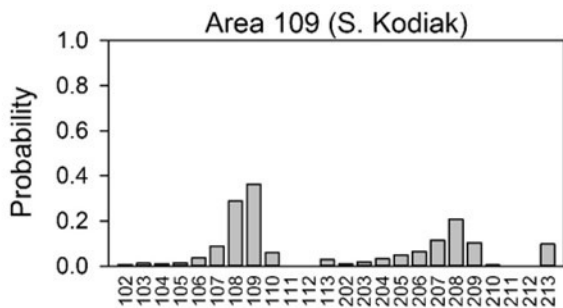
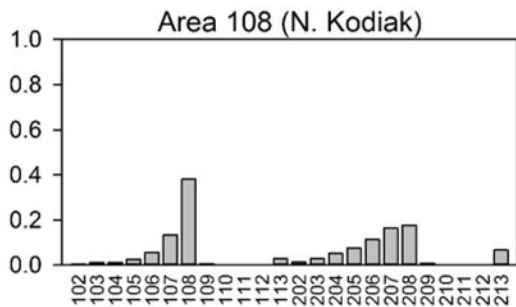
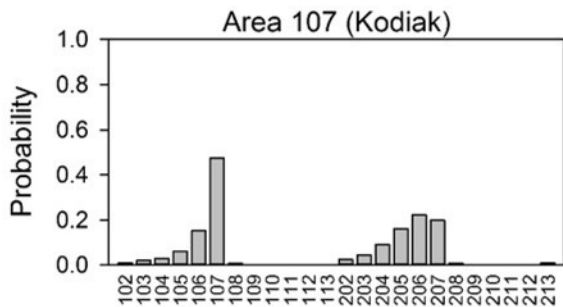
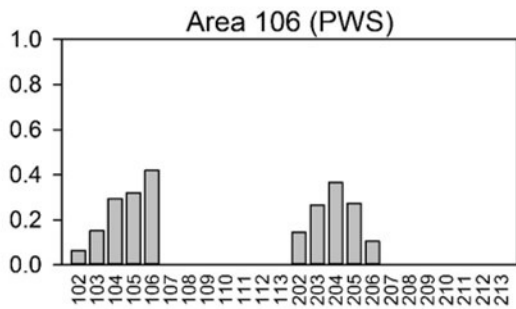
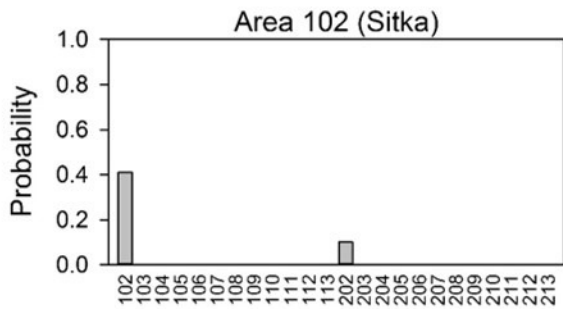






Standard Deviation of Connectivity 1997-2013





Spawning Areas

Spawning Areas

